

## 5 A Novel PDZ Binding Motif

PDZ domains participate in at least four different classes of interactions: recognition of carboxyl-terminal motifs in peptides, recognition of internal motifs ( $\beta$ -finger), PDZ-PDZ dimerization, and recognition of lipids (see Chapter 1.2). In this chapter, a new possible binding motif will be elucidated for the AF6 and the ERBIN PDZ domains, which could be deduced for the 6223-Humlib screens presented in Chapters 3 and 4. This new binding motif represents the canonical C-terminal binding mode but with an additional amino acid at the extremely C-terminus of the peptide ligand. Furthermore, it seems that this ‘elongated’ peptide ligand is still able to interact with the conserved binding groove of the PDZ domain.

This new putative PDZ binding motif is mainly analyzed based on the ERBIN PDZ domain interaction with the C-terminal peptides of the angiotensin II type 2 receptor and rhombotin-1, respectively. *In vitro* screening, using substitutional analyses, combinatorial libraries and SRP measurements gave insight into this new PDZ binding motif, which is confirmed below by *in vivo* co-localization.

### 5.1 Type-2 Angiotensin II Receptor

The octapeptide angiotensin II (Ang II, DRVTIHPF) regulates blood pressure and electrolyte balance, hormone secretion, tissue growth and neuronal activity by interacting with specific receptors on target organs. It acts through at least two types of receptors termed type-1 angiotensin II receptor (AG2R [SP: P30556]) and type-2 angiotensin II receptor (AG22 [SP: P50052]). Both human AG2R and AG22 receptors belong to the G-protein-coupled, seven transmembrane-spanning domain family of receptors, but they only share 32% homology in amino acid sequence [162, 163]. The divergence between AG2R and AG22 receptors is seen in the third intracellular loop and more extensive differences in the C-terminal tail. The AG2R receptor, which mediates most of the known functions of Ang II including effects on the cardiovascular system and fluid and electrolyte homeostasis [164], associates with the  $G\alpha$  subunit of G-proteins. Activation of the AG2R

receptor stimulates phospholipase C-mediated pathways, mitogen-activated protein kinases and protein tyrosine phosphorylation [165, 166].

```

AG22_HUMAN      MKGNSTLATTSKNITSGLHFGLVNIISGNNESTLNCSQK-PSDKHLDAIPILYIIFVIGF
AG22_RABBIT     MKDNFTLAAINRNITGSLHLGLMNFNNGNESALNCSYK-PSDKQLDAIRILYFIFVIGS
AG22_MOUSE      MKDNFSAATSRNITSSRPFDNLNATGTNESAFNC SHK-PSDKHLEAIPVLYYIMFVIGF
AG22_RAT        MKDNFSAATSRNITSSLPFDNLNATGTNESAFNC SHK-PADKHLEAIPVLYYIMFVIGF
AG22_MERUN      MKDNFSAATSRNITSSLPFVNLMNSGTNDLIFNC SHK-PSDKHLEAIPVLYYIIFVIGF
AG22_SHEEP      -----PVLYYIIWGVGF
AG22_EEL        -----MENLTVGRTEGIHITCNTSGRHSYIYTLIPVVYGCNFIYGI
                                     ::*  : :*
                                     -----
                                     TM-1

AG22_HUMAN      LVNIVVVTLFCCQKGPVKVSSIYIFNLAVADLLLLATLPLWATYYSRYDWF LFGPVMCKV
AG22_RABBIT     LVNAVVVTLFCCQKGPVKVSSIYIFNLAVADLLLLATLPLWATYYSRYDWF LFGPVMCKV
AG22_MOUSE      AVNIVVVSLFCCQKGPVKVSSIYIFNLALADLLLLATLPLWATYYSRYDWF LFGPVMCKV
AG22_RAT        AVNIVVVSLFCCQKGPVKVSSIYIFNLAVADLLLLATLPLWATYYSRYDWF LFGPVMCKV
AG22_MERUN      AVNIIVVSLFCCQKGPVKVSSIYIFNLAVADLLLLATLPLWATYYSRYDWF LFGPVMCKV
AG22_SHEEP      LVNTIVVTLFCCQKGPVKVSSIYIFNLAVADLLLLATLPLWATYYSRYDWF LFGPVMCKV
AG22_EEL        VGNSMVVAVIYCYMKLKTVANIFVNLAVS DLTFLITLPMWATFTAMGYNWPFGGLCKA
* :*: : *  * .*: :*: :*: :* : : * :*: :* : : * * * * : : * : *
-----
TM-2

AG22_HUMAN      FGSFLTLMNFASIFFITCMSVDRYQSVIYPFLS-QRRNPWQASYIVPLVWCMACLSLPT
AG22_RABBIT     FGSFLTLMNFASIFFITCMSVDRYQSVIYPFLS-QRRNPWQASYIVPLVWCMACLSLPT
AG22_MOUSE      FGSFLTLMNFASIFFITCMSVDRYQSVIYPFLS-QRRNPWQASYVVPVWCMACLSLPT
AG22_RAT        FGSFLTLMNFASIFFITCMSVDRYQSVIYPFLS-QRRNPWQASYVVPVWCMACLSLPT
AG22_MERUN      FGSFLTLMNFASIFFITCMSVDRYQSVIYPFLS-QRRNPWQASYVVPVWCMACLSLPT
AG22_SHEEP      FGSFLTLMNFASIFFITCMSVDRYQSVIYPFLS-QRRNPWQASYIVPLGWCMACLSLPT
AG22_EEL        SAGLTI FNLYTSIFFLTSLSIDRYLAIVHPVRSRQRRTVVYARITCVLIWAFALSLPT
.. : :*: :*: :* :* :* :* :* :* :* :* :* :* :* :* :* :* :* :* :*
-----
TM-3                                     TM-4

AG22_HUMAN      FYFRDVRTIEYLGVNACIMAFPPPEKYAQWSAGIALMKNILGFI I PLIF IATCYFGIRKHL
AG22_RABBIT     FYFRDVRTIDYLGVNACIMAFPPPEKYAQWSAGIALMKNILGFI I PLIF IATCYFGIRKHL
AG22_MOUSE      FYFRDVRTIEYLGVNACIMAFPPPEKYAQWSAGIALMKNILGFI I PLIF IATCYFGIRKHL
AG22_RAT        FYFRDVRTIEYLGVNACIMAFPPPEKYAQWSAGIALMKNILGFI I PLIF IATCYFGIRKHL
AG22_MERUN      FYFRDVRTIEYLGVNACVMAFPPPEKYAQWSAGIALMKNILGFI I PLIF IATCYFGIRKHL
AG22_SHEEP      FYFRDVRTIEYLGVNACIMAFPPPEKYAQWSAGIALMKNILGFI I PLIF IATCYFGIRKHL
AG22_EEL        ALSRDVFTINHPTTVCG-TL DKHEL SHVLVAIGLMKSVLGFLIPFVI IVTCYCLIGRAL
*** ** : : . . . * : : : : . . * . * . * : * : * : * : * : * : *
-----
TM-5

AG22_HUMAN      LKTNSYGKNRITRDQVLKMAAAVVLAFI ICWLPFHVLTFLDALAWMGVINSCEVIAVIDL
AG22_RABBIT     LKTNSYGKNRVTRDQVLKMAAAVVLAFI ICWLPFHVLTFLDALTWMGVINSCEVTAVIDL
AG22_MOUSE      LKTNSYGKNRITRDQVLKMAAAVVLAFI ICWLPFHVLTFLDALTWMI INSCEVIAVIDL
AG22_RAT        LKTNSYGKNRITRDQVLKMAAAVVLAFI ICWLPFHVLTFLDALTWMI INSCEVIAVIDL
AG22_MERUN      LKTNSYGKNRITRDQVLKMAAAVVLAFI ICWLPFHVLTFLDALSWMGI INSCEVMAVIDL
AG22_SHEEP      LKTNSYGKNRITRDQVLKMAAAVVLAFI ICWLPFHVLTFLDALAWMGVINSCEVIAVIDL
AG22_EEL        LEARRVQSSRSRGDEVLQMLAAVLAFLFCWVPHQIFHFHMHVLALLKVIENCP TLDI IDT
* : : . . . * : * : * : * : * : * : * : * : * : * : * : * : * : *
-----
TM-6

AG22_HUMAN      ALPFAILLGFTNSCVNPFYCFVGNRFQOKLRSVFRVP-----ITWLQ GKRESMSR
AG22_RABBIT     ALPFAILLGFTNSCVNPFYCFVGNRFQOKLRSVFRVP-----ITWLQ GKRESMSR
AG22_MOUSE      ALPFAILLGFTNSCVNPFYCFVGNRFQOKLRSVFRVP-----ITWLQ GKRETMSR
AG22_RAT        ALPFAILLGFTNSCVNPFYCFVGNRFQOKLRSVFRVP-----ITWLQ GKRETMSR
AG22_MERUN      ALPFAILLGFTNSCVNPFYCFVGNRFQOKLRSVFRVP-----ITWLQ GKRETMSR
AG22_SHEEP      ALPFAILLG-----
AG22_EEL        ALPFTICIA YFNSCMNP ILYGFVGRNFRRLRLRLRCGPGSAAARHSHPSLTTKMSTLSYR
*** : * : .
-----
TM-7

AG22_HUMAN      KSSSLREMETFVS-----
AG22_RABBIT     KSSSLREMETFVS-----
AG22_MOUSE      KGSSLREMDTFVS-----
AG22_RAT        KSSSLREMDTFVS-----
AG22_MERUN      KSSSLREMDTFVS-----
AG22_SHEEP      -----
AG22_EEL        ASETLRLTSGKAASSQPAK

```

**Figure 5.1 Sequence Alignment of AG22 Homologues.**

The homologues of the human AG22 were searched using PIR-NREF database and the obtained homologous sequences were aligned using BLAST.

The open reading frame of the AG22 cDNA encodes 363 amino acid residues with 99% sequence identity between rat and mouse, and 72% identity between rat and human. The divergence between the rodent and human AG22 occurs mainly in the N-terminus [167] (Figure 5.1).

The actions of the AG22 receptor and its intracellular signaling pathways are being elucidated. This subtype is highly expressed in fetal tissues, whereas its expression is dramatically decreased after birth and restricted only to a few organs such as the brain, adrenal, heart, myometrium and ovary. The AG22 receptor is re-expressed in the adult animal after cardiac and vascular injury, and nerve crush, and during wound healing or kidney obstruction. This suggests a role for this receptor in tissue remodeling, growth and/or development [168]. Interestingly, AG22 receptor knockout mice show no major morphological abnormalities but display alterations in blood pressure control and behavior [169, 170].

### 5.1.1 Signaling Pathway Activated by the AG22 Receptor

Although structurally related to G-protein-coupled receptors, the AG22 receptor displays atypical signal transduction and G-protein-coupling mechanisms [171]. While early studies led to disparate and mostly controversial results, it is now becoming clear that AG22 activates three major cascades of intracellular events: 1. activation of protein phosphatases and protein dephosphorylation, 2. regulation of the nitric oxide (NO)-cGMP system and 3. stimulation of phospholipase A2 (PLA2) and release of arachidonic acid (Figure 5.2) (reviewed in [168, 172]). Depending on the cell type and signal pathway examined, the AG22 receptor has been reported to couple to  $G\alpha_i$  [173, 174] or to still unknown G-proteins [175, 176]. Furthermore, ceramide, which is linked to phosphatase activation, was proposed to be the second messenger in AG22 receptor mediated apoptosis [177, 178].

In cultured hypothalamic neurons, the AG22 receptor-mediated delayer rectifier  $K^+$  current is abolished [179]. Furthermore, AG22 receptor-stimulated activation of the protein phosphatase 2A (PP2A) has also been shown. PP2A activation results in dephosphorylation and inactivation of growth factor activated mitogen-activated protein kinase (MAPK) and, in particular, inactivation of extracellular signal-regulated kinase (ERK1/2) [180]. The AG22 receptor promotes apoptosis through stimulation of ERK

phosphatases, which is in turn associated with dephosphorylation and inhibition of MAPK and Bcl-2 [181]. Interestingly, AG22 receptor effects on MAPK are cell-specific. For example, in renal proximal tubular epithelial cells, AG22 receptor activation results in membrane-associated PLA2 activation or protein-tyrosine phosphatase (PTP) inhibition, respectively, this in turn leads to MAPK activation [182].

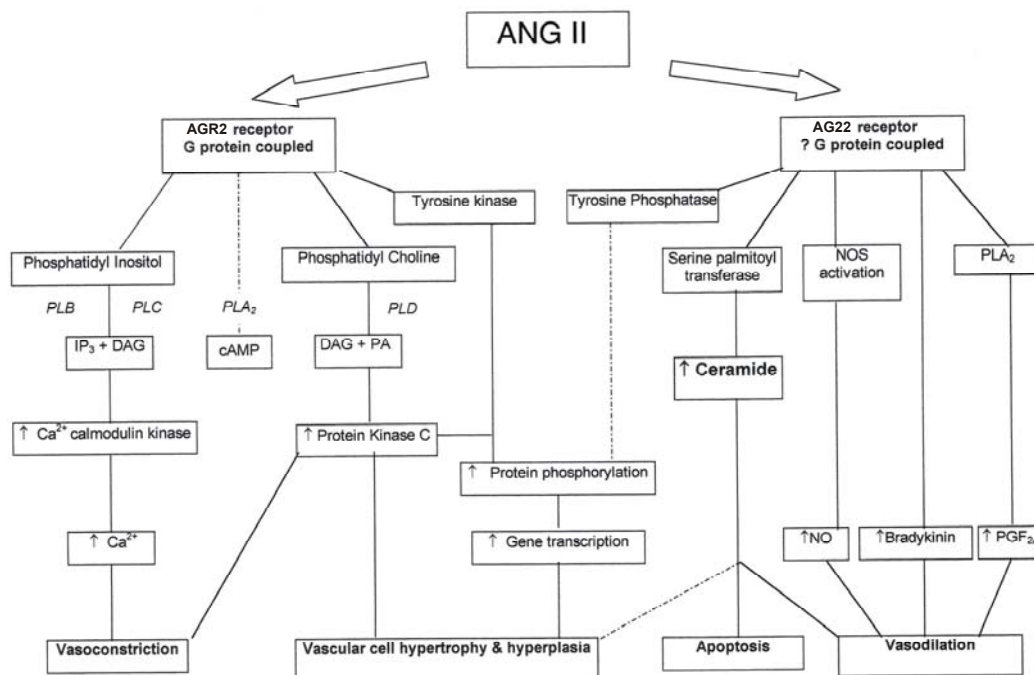


**Figure 5.2 Signal Mechanism and Physiological Effects of AG2R and AG22 Receptor.**

NOS, nitric oxide synthase; PLA<sub>2</sub>, PLB, and PLD, phospholipase A<sub>2</sub>, B, and D, respectively; PGF<sub>2</sub>, prostaglandin F<sub>2</sub>; DAG, diacylglycerol; PA, phosphatidic acid.

### 5.1.2 Negative Crosstalk between AG2R and AG22 Receptor Subtypes

In numerous studies, including knockout experiments, the AG22 receptor has been shown to counteract the effects of Ang II mediated by the AG2R receptor, suggesting that AG22 might provide a brake for hormonal signal. The heterodimers of both AG22 and AG2R exhibit impaired Ang II signaling implying an antagonist function of AG22 on AG2R [183]. Additionally, several studies have found opposite intracellular effects of the AG2R and AG22 receptors, particularly on the regulation of protein kinases and phosphorylation [184, 185]. Since Ang II binds to its two receptor subtypes AG2R and AG22 with similar affinity, the cellular response is highly dependent on the relative expression level and/or

responsiveness of both receptors. Preliminary results tend to indicate that AG22 receptor expression is upregulated upon prolonged Ang II stimulation. Unlike the AG2R subtype, AG22 does not seem to internalize after ligand binding [186], and so far it is not known whether its response can be attenuated by desensitization.

## 5.2 Rhombotin-1

Rhombotin-1 is a protein containing only LIM domains and plays a critical role in development. It is a member of the family of the LIM-only (LMO) proteins. Rhombotin-2 (LMO2), as an other example, is essential for hematopoiesis and thus for the survival of the mouse [193], but biochemical functions of the LMOs are not clear.

### 5.2.1 LIM Domains

The LIM domain contains a cysteine-rich motif that was first identified in, and named after, the protein products of three regulatory genes, lin-11, isl1, and mec-3 [187, 188]. The LIM motif is basically composed of two zinc finger structures separated by a two-amino acid spacer and conforms to the consensus sequence  $(C_{x_2}C_{x_{(16-23)}}(H/C/D)_{x_2}(C/E/H)_{x_2}C_{x_2}C_{x_{(16-21)}}(C/H/D)$  [189-191].

Many of the LIM-containing proteins appear to function in cell differentiation, lineage determination and body pattern formation during embryogenesis. Four class-types of LIM proteins are known: One class features DNA-homeodomain (HD) motifs, the second class includes 'LIM-only' proteins, the third class contains proteins with C-terminal LIM motifs in addition to other structural modules and the fourth class comprises proteins with N-terminal LIM motifs as well as other C-terminal motifs [192].

Although LIM-containing proteins are clearly important for developmental regulation and cell differentiation, the functions of the proteins at molecular level are not well understood. Taken together, LIM domains are multiple binding and adapter modules, which mediate interactions with a variety of proteins through their additional motifs or through homo- and/or heterodimerization.

### 5.2.2 Rhombotin-1

The genes encoding the rhombotin-1 (LMO1) and rhombotin-2 (LMO2) proteins were discovered as transcription units adjunct to the breakpoints of chromosomal translocations t(11;14)(p15;q11) and t(11;14)(p13;q11), respectively [194]. The chromosomal translocations activating LMO1 and LMO2 are found only in T cell tumors and it seems likely that epitopic expression of the LIM-proteins contributes to leukaemogenesis by the ability to form aberrant protein associations in T cells [195].

## 5.3 Results

### 5.3.1 Novel Binding Specificity for PDZ Domains

The screen extent of the 6223 human C-terminal peptide library using the AF6 and the ERBIN PDZ domains revealed the canonical PDZ binding motifs  $(\pi/E)(\psi/T/S)x\psi_{\text{COOH}}$  and  $(E/D)(T/S/V)x(V/L/I)_{\text{COOH}}$  for each PDZ domain, respectively (see Chapter 4). Besides this conventional motif, which included the last four C-terminal amino acids and the free carboxyl group, we observed a new binding mode, which we denoted ‘shifted motif’. This shifted motif is defined by the conventional PDZ domain-binding motif with an additional amino acid after position 0 (named hereafter position +1). The angiotensin II type 2 receptor (AG22, C-terminal peptide SSLREMETFVS<sub>COOH</sub>) was detected for both PDZ domains and, additionally, rhombotin-1 (RHM1, C-terminal peptide QLNGTFESQVQ<sub>COOH</sub>) for the ERBIN PDZ domain. The substitutional analyses of both peptide sequences show that position +1 could be replaced by any of the other 19 amino acids (cysteine omitted), demonstrating that this position is not a key residue for the PDZ domain/ligand interaction (Figure 5.3, first and second panel).

The substitutional analysis of AG22 without S at position +1 reveals the same substitutional pattern for position 0 through -3 as the peptide with S, indicating that position +1 did not essentially contribute to the binding specificity of this peptide (Figure 5.3, third panel).

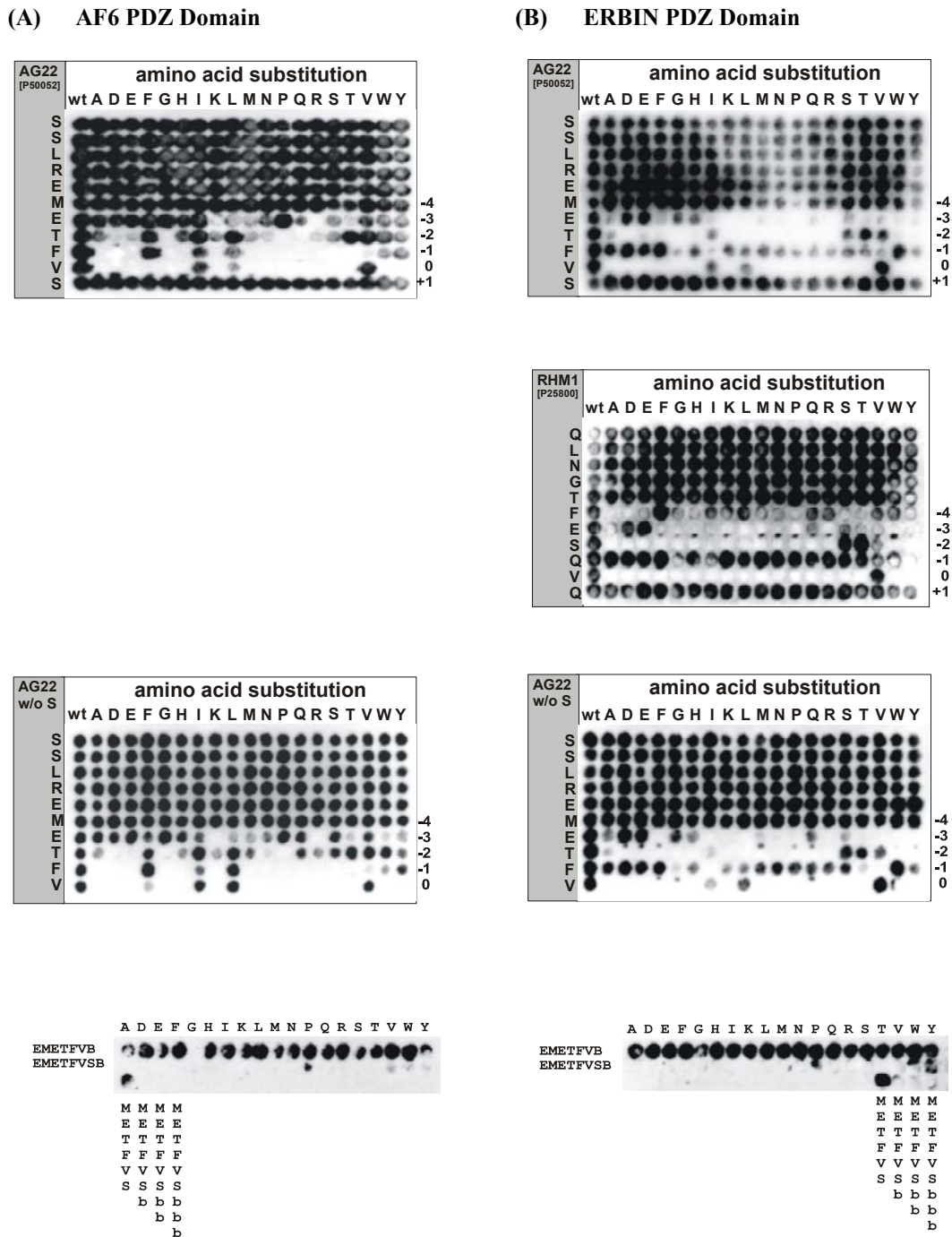


**Figure 5.3 Characterization of PDZ Domain Ligands with the Shifted Motif.**

The substitutional patterns showed that the four C-terminal positions 0 through -3 are specific for the binding of the shifted motif to the AF6 and ERBIN PDZ domains. Furthermore, only one C-terminal amino acid (position +1) could be insert in the PDZ domain binding pocket. Additional amino acids (position above position +1) disrupted the PDZ domain/ligand interaction.

(A) GST-AF6 and (B) GST-ERBIN PDZ domain incubation.

First panel - substitutional analyses of AG22: SSLREMETFV<sub>COOH</sub>; second panel - substitutional analyses of RHM1: QLNGTFESQVQ<sub>COOH</sub>; third panel - substitutional analyses of AG22 without serine at position +1; fourth panel - influence of the C-terminal amino acids.

All spots in the left hand columns (grey box) are identical and represent the wild type (wt) peptide. All other spots are single substitution analogues, with the rows defining the sequence position that is substituted and the columns defining the amino acid used as a replacement. B: permuted position with all 19 amino acids without cysteine; b: mixture of 17 L-amino acids without C, M and W.

The importance of position +1 was examined by a variation of different analyses, which include additional amino acids at the C-terminus of the peptide sequence of AG22 (Figure 5.3, fourth panel). To find out how many amino acids could be added after position 0, the shorter peptide sequences METFVSCO<sub>OH</sub> of AG22 were synthesized with additional amino acid mixtures 'x' (up to 3). Simultaneously, the 7mer sequence of AG22 (EMETFVSCO<sub>OH</sub>) was subjected to an amino acid permutation at position +1 and at the notional position +2. As shown in the substitutional analyses, only position +1 could be substituted with all 19 amino acids, whereas the binding was abolished by the incorporation of an additional amino acid above position +1.

In both cases, the C-terminal peptide sequences of AG22 and RHM1 have a valine at position 0. To examine the dependence of the amino acids in position 0 and +1, a combinatorial library of the type EMETFB<sub>0</sub>B<sub>+1</sub>CO<sub>OH</sub> was synthesized and incubated with the AF6 and the ERBIN PDZ domains, respectively (Figure 5.4). Besides some other single combinations, we observed that valine in position 0 is always present independently of the amino acid type in position +1.

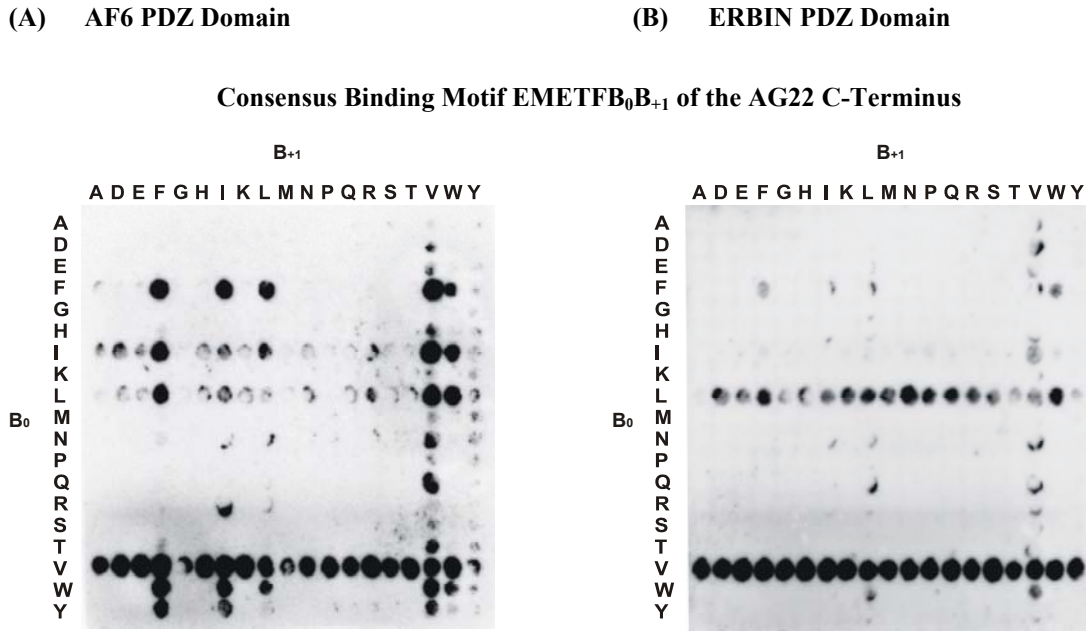


**Figure 5.4 Simultaneous Substitution of two Amino Acids in the C-Terminal Sequence Motif of AG22.**

(A) GST-AF6 and (B) GST-ERBIN PDZ domain incubation of the combinatorial library of EMETFB<sub>0</sub>B<sub>+1</sub>CO<sub>OH</sub>. An additionally amino acid in position +1 is especially tolerated if V is present at position 0. (B: permuted position with all 19 amino acids without cysteine, b: mixture of all 17 L-amino acids without C, M and W.)



### 5.3.2 PDZ Domain/AG22 Peptide Interaction Determined by NMR and SPR

Based on the assignment of the backbone  $^1\text{H}$ - $^{15}\text{N}$  resonances of the AF6 PDZ domain, which was described in Chapter 4, the interactions of the AF6 PDZ domain and the C-terminal peptide of the AG22 receptor were analyzed by NMR. Unfortunately, only small chemical shifts were observed at a 8-fold excess of the peptide in comparison to the AF6 PDZ domain concentration, implying an unspecific interaction. Additionally, the determination of the  $K_d$  using SPR measurements of the same interaction is not reproducible and could only be estimated (78.9  $\mu\text{M}$  - 287.3  $\mu\text{M}$ ).

On the other hand, SPR measurements of the ERBIN PDZ/AG22 peptide complex exhibit a  $K_d$  of 105.4  $\mu\text{M}$  (95.5  $\mu\text{M}$  - 116.4  $\mu\text{M}$ ). This result gives us the opportunity to clarify this interaction structurally by molecular modeling, as described in the following chapter.

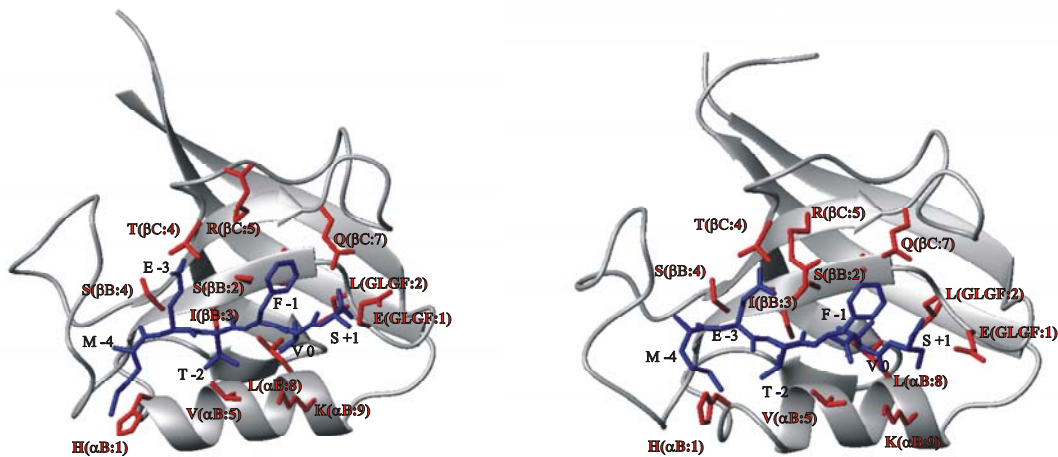
### 5.3.3 Modeling of the PDZ Domain/Shifted Motif Complex

One of the most commonly used force fields for protein simulations is AMBER (Assisted Model Building with Energy Refinement) [123]. It is used to study protein folding, to analyze the relative free energies of the binding of two ligands to a given host (or two hosts to a given ligand), to investigate the sequence-dependent stability of proteins and nucleic acids, and to find the relative solvation free energies of different molecules in various liquids.

The crystal structure of the ERBIN PDZ domain (1MFG) [122] has been chosen for the structural analysis of the ERBIN PDZ domain/AG22 complex by molecular dynamics. The original peptide ligand ERB2 present in 1MFG is replaced by the C-terminal peptide sequences of AG22 (METFVS<sub>COOH</sub>), which is placed in the PDZ binding groove analogous to the ligand in 1QAV ( $\beta$ -finger binding mode of the nNOS/syntrophin complex) [16]. This starting structure, called hereafter **1MFGtemp**, was subjected to molecular dynamic simulations (including solvation and minimization) resulting in the **1MFGmd** model. Compared to the usual peptide ligand placement in the PDZ domain binding groove, the backbone of the ligand of **1MFGtemp** was displaced away from the binding groove in direction of the solvent, to allow the conserved PDZ domain/ligand contacts and enough

space for an additional amino acid (position +1) at the C-terminus (Figure 5.5 (A), left side). The C-terminal peptide of AG22 was placed into the PDZ domain-binding pocket based on the peptide ligand location of the solved PDZ domain complexes in the PDB database. In spite of this fact, the surface representation reveals a possible clash of the serine in ligand position +1 and the GLGF-loop, especially with E (GLGF:2) of the PDZ domain (Figure 5.5, (B), left side).

(A)



(B)

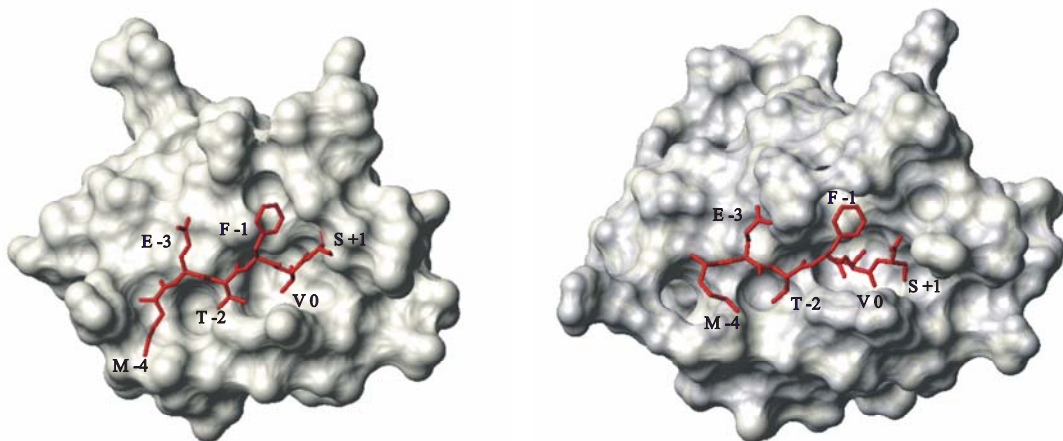


**Figure 5.5 Structural Description of the ERBIN PDZ Domain with the C-terminal AG22 Peptide.**

(A) Ribbon representation of 1MFGtemp (left side) and of 1MFGmd (right side) in complex with the C-terminal peptide of AG22 (METFVSCOOH) (colored in blue) denoted with position -4 through +1. The side chains of the PDZ domain interacting with the ligand are shown in red color and are labeled after our PDZ domain nomenclature (see Chapter 2.1.1)

(B) Surface representation of 1MFGtemp (left side) and of 1MFGmd (right side) in complex with the C-terminal peptide of AG22 (METFVSCOOH) (colored in red) denoted with position -4 through +1.

After the MD simulation, the carboxyl group of S in ligand position +1 is forced into IA<sub>0</sub> displacing the ligand to the left (3.07 Å between of S<sub>Cα</sub>(1MFG**temp**) and S<sub>Cα</sub>(1MFG**md**)). Furthermore, this provokes a little twist between the C<sub>α</sub> and the NH of the V backbone (ligand position 0) displacing it deeper in IA<sub>0</sub> (2.17 Å from V<sub>Cα</sub>(1MFG**temp**) to V<sub>Cα</sub>(1MFG**md**)). Due to this twist, the movement of the upstream amino acids diminish from one amino acid to the next (1.15 Å from F<sub>Cα</sub>(1MFG**temp**) to F<sub>Cα</sub>(1MFG**md**), 0.99 Å from T<sub>Cα</sub>(1MFG**temp**) to T<sub>Cα</sub>(1MFG**md**) and 0.91 Å from E<sub>Cα</sub>(1MFG**temp**) to E<sub>Cα</sub>(1MFG**md**)). Taken together, the C-terminal ligand of AG22 retains its particular relation between ligand positions/interaction areas after the MD simulation even with the additional amino acid in position +1.

The residues of the PDZ domain that differed to the greatest extent from the starting conformation were in the loop between the βB- and the βC-strands and near the C- and N-terminus (Figure 5.7). The long amino acid side chains of the PDZ domain E(βB:1), R(βC:5), Q(βC:7) move in the direction of the ligand and clamp it into the binding pocket (Figure 5.5 and Figure 5.7).

H-bond calculations using MolMol revealed the following four H-bonds within the model of 1MFG**temp**: 1. between the hydroxyl group of S at ligand position +1 and the amino group of G (GLFG:3); 2. between the carbonyl group of V at ligand position 0 and the amino group of G (GLFG:3); 3. between the carbonyl group of T at ligand position -2 and the amide group of I (βB:3) and 4. between the amino group of T at ligand position -2 and the carbonyl group of I (βB:3). After MD simulation the 1MFG**md** model likewise exhibits four H-bonds, namely: 1. between the hydroxyl group of S at ligand position +1 and the amino group of L (GLFG:2); 2. between the hydroxyl group of S at ligand position +1 and the amino group of G (GLFG:3); 3. between the amino group of V at ligand position 0 and the carbonyl group of F (βB:1) and 4. between the amino group of T at ligand position -2 and the carbonyl group of I (βB:3). Both models show the same amount of H-bonds indicating that both molecules display the same stability factor.

### 5.3.4 ERBIN/AG22 Co-Localization

To explore the interaction between the ERBIN PDZ domain and AG22 *in vivo*, the full-length ERBIN protein and the whole AG22 receptor were used for co-localization assays.

In a first experiment, the full-length ERBIN and AG22 proteins were overexpressed alone in HEK292 cells to determine their cellular expression patterns. The ERBIN protein was mainly expressed in the cytosol, whereas the AG22 expression pattern seemed to be dependent on the Ang II stimulation. AG22 was expressed membrane compartment throughout the whole cell without Ang II stimulation and, in contrast, mainly on the cell surface after stimulation with a 100 nM Ang II solution.

The immunofluorescence (IF) of ERBIN and AG22 showed that ERBIN co-localized with AG22 in HEK293 cells (Figure 5.6). Additionally, we overexpressed the C-terminal peptide of AG22 (GFP-AG22<sub>Cterm</sub>) in order to observe a suppression of the ERBIN/AG22 interaction. Nevertheless, the overlay of the three expression patterns revealed only an ERBIN/AG22 co-localization without an influence of the GFP-AG22<sub>Cterm</sub>.

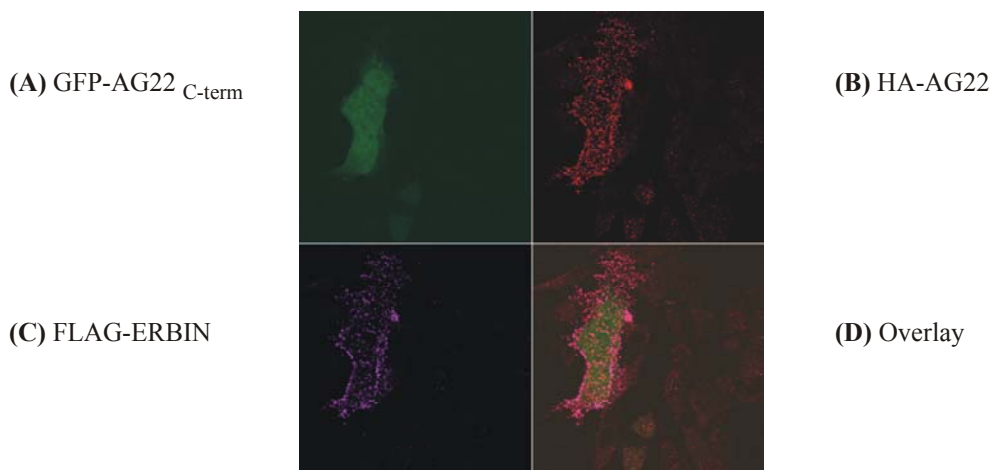


**Figure 5.6 Co-localization of ERBIN with AG22 in Presence of the C-Terminal Peptide of AG22 (AG22<sub>Cterm</sub>).**

Confluent HEK293 cells were transfected with GFP-AG22<sub>Cterm</sub>, HA-AG22 and FLAG-ERBIN. GFP-AG22<sub>Cterm</sub> could be directly detected (A) whereas AG22 and ERBIN were visualized by doubly immunostaining using (B) polyclonal rabbit anti-HA/anti-rabbit-cy3 for AG22 and (C) monoclonal mouse anti-FLAG/anti-mouse-cy5. (D) Overlay of the three pictures (A-C).

## 5.4 Discussion

### 5.4.1 The Shifted Motif as a New PDZ Domain/Ligand Recognition Mode

Based on the data of both 6223-Humlib screens, a potential new binding mode for the AF6 and the ERBIN PDZ domains is observed, which is also present in the first PDZ domain screen of Hoffmüller *et al.* [104]. The so-called shifted motif E(S/T)xVx<sub>COOH</sub> reveals the possible incorporation of an additional amino acid at the extreme C-terminus of the ligand. The different analyses of the AG22 C-terminal peptide with both PDZ domains and of the RHM1 C-terminal peptide with the ERBIN PDZ domain (substitutional analyses, incorporation and deletion of amino acids at the C-terminus, combinatorial libraries) confirm the specificity of these interactions. Only one additional amino acid at ligand position +1 has enough places in the interaction area 0 (IA<sub>0</sub>) of the PDZ domain besides the amino acid at ligand position 0. Each type of amino acid could be introduced at position +1, as long as V is present at position 0, whereas additional amino acids in position +2 or +3 abolish the PDZ domain/ligand interaction. Taken together, these results allow speculation that the interaction between the ‘shifted motif’ and the PDZ domain are probably similar to the canonical PDZ domain/ligand C-termini interaction, but rather distinguished from the known PDZ domain/ $\beta$ -finger interaction.

Unfortunately, the interaction between the AF6 PDZ domain and the C-terminal peptide of AG22 analyzed by NMR titrations and SPR measurements revealed no chemical shift changes and hard-to-measure  $K_d$  values, respectively. Further investigations, such as the verification of the intactness of the protein structure by 1D-NMR and of the ligand sequence by MS, revealed no particularities questioning the specificity of this interaction. Further *in vitro* and/or *in vivo* experiments should be done to quantify the specificity of the AF6 PDZ domain/shifted motif interaction.

On the other hand, the  $K_d$  value of the ERBIN PDZ domain/AG22 peptide interaction of about 105.4  $\mu$ M (95.5  $\mu$ M - 116.4  $\mu$ M) and the stable complex after the MD simulation demonstrated that the shifted motif could be a putative binding mode for the ERBIN PDZ domain. In vacuum simulations, charged side chains frequently collapse on the surface, forming salt bridges with other charged surface residues, whereas in simulations with explicit solvent, charged side chains frequently stick out, solvated by the solvent dipoles.

After the simulation in water, the ERBIN PDZ domain/AG22 peptide complex is not disrupted and, furthermore, the conserved side chains of the PDZ domain, interacting with the ligand, moved and maintained the ligand more steadily in the binding groove. The ligand is relocated deeper in the binding pocket of the PDZ domain first of all in IA<sub>0</sub> till IA<sub>-3</sub>, while in IA<sub>-4</sub> the ligand seems to have fewer contacts to the PDZ domain (Figure 5.7). However, this latter position contributes generally only to a minor part of the total binding specificity of PDZ domains (see Chapter 4).

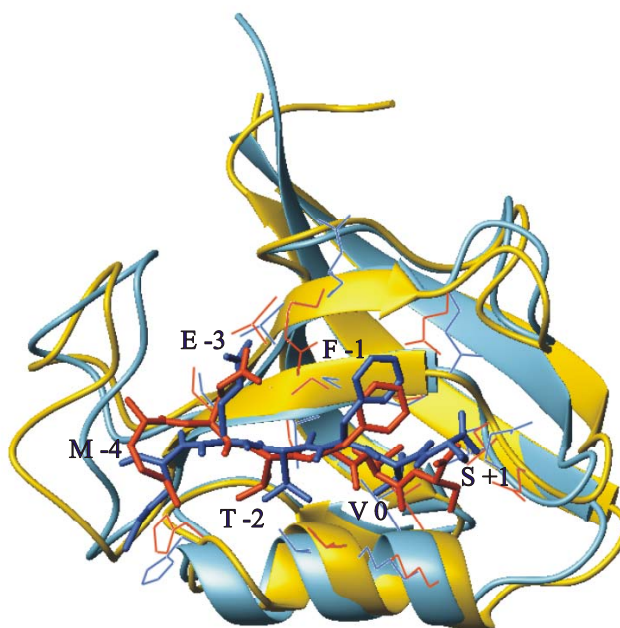


**Figure 5.7** Overlay of the ERBIN PDZ Domains with the C-Terminal AG22 Peptides.

The ribbon models represent an overlay of 1MFGtemp (blue ribbon model, with blue ligand) and 1MFGmd (yellow ribbon model with orange ligand), both with the ligand AG22 (METFVSCOOH) denoted with position -4 through +1. Remarkable conformation changes are only observed in the flexible region, like the C- and N-terminus and the loops.

To validate our MD simulations, the backbone RMSD values of the 1MFG model compared to the 2PDZ (canonical SNA1 PDZ binding mode) [34] and to the 1QAV ( $\beta$ -finger binding mode of SNA1) [16] structures, respectively, are determined (Table 5.1). The values of 1MFG after the minimization are in accordance with 1QAV, which was the basis of the AG22 C-terminal ligand modeling, but after the MD simulation the values fit with the 2PDZ model. This result, which is coincident with the average of the backbone RMSD values of the conserved PDZ domain/ligand placement (from 0.86 Å to 1.95 Å, see

Chapter 4), shows that the C-terminal shifted motif is not a putative  $\beta$ -finger binding mode.

**Table 5.1** Backbone RMSD Values of 1MFG Compared with 2PDZ and 1QAV.

	Minimization		MD Simulation	
	2PDZ	1QAV	2PDZ	1QAV
<b>Ca</b>	0.80	0,67	1,35	2,18
<b>CaCb</b>	0.80	0,73	1,43	2,22
<b>BB</b>	1,09	0,69	1,77	2,63
<b>SC</b>	1,89	0,54	2,09	2,44

**Footnotes:** Backbone RMSD for the  $C\alpha$ , the  $C\beta$ , the backbone without hydrogen atoms (BB) and the side chains (SC). First values are the RMSD of 1MFG after the minimization and the second values those after the MD simulation.

The amino acids in ligand position 0 through -3 contribute the main part of the total affinity in the PDZ domain/ligand complex. In case of the ERBIN PDZ domain, the peptide sequence ET(W/F)V<sub>COOH</sub> represents the four favorite C-terminal amino acids of the ligand ( $K_d \sim 1 \mu\text{M}$ , equal to the super-binder, see also Chapter 4.3.6). An additional amino acid in position +1 will probably reduce the  $K_d$  value to a factor of 10-15, which is still in a range of a specific affinity. The ERBIN PDZ domain probably tolerates ligands with the shifted motif only if the other positions are occupied with the optimal amino acids, allowing a higher divergence in the recognition of their target sequence space.

The *in vitro* collected data, especially for the ERBIN PDZ domain/AG22 peptide interaction, were validated by *in vivo* co-localization experiments. The full-length ERBIN co-localize with the AG22 receptor at the cell membrane. The GFP-AG22<sub>Cterm</sub>, which was co-expressed to display the ERBIN/AG22 interaction, does not influence this interaction. The full-length proteins of ERBIN and AG22 could presumably accomplish more contacts between them than the canonical PDZ domain/receptor interaction. These contacts may contribute to the binding affinity by increasing the  $K_d$  value. To validate the specificity of this interaction, further analyzes have to be performed using for example, a GFP-tagged peptide with a lower  $K_d$  (such as GFP-APC,  $K_d = 19.2 \mu\text{M}$  (18.2  $\mu\text{M}$  - 20.3  $\mu\text{M}$ )) or using a C-terminal mutated AG22 receptor as negative control or by additional *in vivo* experiments.

## 5.4.2 Biological Relevance

### 5.4.2.1 The ERBIN PDZ Domain and AG22

Although the components of the EGFR pathway are known, much less is known about the fine-tuning of the pathway and how cross-talk with other pathways is regulated. A recent paper by Huang *et al.* [73] sheds new light on the former issue and raises some provocative possibilities regarding the latter. The authors show that ERBIN suppresses ERK (extracellular signal-regulated kinase) activation by interference with the activation of Raf-1 by Ras-GTP. Ras can be locked in an incomplete hydrolysis of the associated GTP. Such mutations result in an oncogenic Ras protein that is a hallmark of many human cancers. ERBIN binds selectively to mutational activated Ras and blocks its interaction with Raf-1, thereby abolishing Ras activation of Raf-1 and the ERK pathway. Inhibition of the ERK pathway requires the LRRs, but not the PDZ domain. LRRs mediate protein interactions and have previously been identified as Ras binding motifs, for instance in Sur-8 and RSP1 [Ras suppressor protein 1, also known as RSU1 (Ras suppressor 1)].

The biological relevance of the ERBIN PDZ domain interaction with the AG22 receptor can be deduced from the fact that both proteins act on the MAPK pathway. ERBIN suppresses the MAPK pathway, as described above, by blocking Ras, whereas AG22, depending on its cell expression, could act on this pathway as activator or inhibitor. The molecular relevance of this interaction and/or the influence of the MAPK pathway should be further analyzed by detailed *in vivo* experiments.

### 5.4.2.2 PDZ Domains and LIM Domains

An interaction of a PDZ domain and the C-terminus of a LIM domain containing protein is exemplified *in vitro* and *in vivo* by the second PDZ domain of the human protein-tyrosine phosphatase 1E (hPTP1E) and the zyxin-related protein (ZRP-1, sequence VTTDC<sub>COOH</sub>) [196]. Similar observations have been made in the course of a study of the interaction of the Reversion-Induced LIM protein (RIL, sequence VELV<sub>COOH</sub>), with the protein tyrosine phosphatase (PTP-BL), the mouse homologue of the hPTP1E [197]. The RIL protein interacts with both the PDZ2 and PDZ4 domains, whereby the interaction with PDZ4 is much stronger in the presence of the LIM domains. This observation, which is also seen



between hPRP1E/ZRP-1, suggests that the LIM domains are also playing an important role in stabilizing the interaction with the PDZ domain.

The herein reported interaction between the ERBIN PDZ domain and the C-terminal peptide of the rhombotin-1 (sequence ESQVS<sub>COOH</sub>) likewise shows an unconventional C-terminal ligand motif. All these observations suggest that other C-terminal sequences could also define the specificity for particular PDZ domains. The role of the second LIM domain (aa 88 through 147) of the rhombotin-1 protein (156 aa in total) could have an analogous influence on the binding specificity, which has to be clarified by further studies.